Original Research

Prediction of ovarian aging using ovarian expression of BMP15, GDF9, and C-KIT

Min Jung Park[1,*], Jun-Woo Ahn[2,*], Ki Hyung Kim[3], Junghee Bang[4], Seung Chul Kim[3], Jae Yi Jeong[5], Ye Eun Choi[5], Chang-Woon Kim[5,**] and Bo Sun Joo[1,4,**] (iD)

[1]Korea Institute for Public Sperm Bank, Busan 49241, Korea; [2]Department of Obstetrics and Gynecology, College of Medicine, Ulsan University Hospital, Ulsan 44033, Korea; [3]Department of Obstetrics and Gynecology, Pusan National University School of Medicine, Pusan National University Hospital, Busan 49241, Korea; [4]Department of Cardiothoracic Surgery, Dong-A University Hospital, Busan 602-812, Korea; [5]Department of Obstetrics and Gynecology, Sungkyunkwan University School of Medicine, 51353 Changwon, Korea
Corresponding authors: Bo Sun Joo. Email: bosunjoo@hanmail.net; Chang-Woon Kim. Email: kcwoon@naver.com
*These authors contributed equally to this study and should be considered co-first authors.
**These authors contributed equally to this study and should be considered co-corresponding authors.

Impact statement

Ovarian aging is becoming a more important issue in terms of fertility preservation and infertility treatment. Serum anti-Mullerian hormone (AMH) level and antral follicle count (AFC) are being practically used as markers of ovarian aging as well as ovarian reserve in human. However, these factors have some drawbacks in assessing ovarian aging and reserve. Therefore, the identification of ovarian expressions of BMP15, GDF9, and C-KIT according to female could be applied as a potent predictor of ovarian aging. This work provides new information on the development of diagnosis and treatment strategy of age-related fertility decline and premature ovarian insufficiency.

Abstract

This study investigated ovarian expressions of bone morphogenetic protein 15 (BMP15), growth differentiation factor 9 (GDF9), and C-KIT according to age in female mice to determine whether these factors can be served as new potential biomarkers of ovarian aging. Ovaries were collected from mice aged 10, 20, 30, and 40 weeks, and ovarian expressions of BMP15, GDF9, and C-KIT were examined by real-time PCR, Western blot, and immunohistochemistry. Follicle counts were measured on histological hematoxylin and eosin staining. In the second experiment to evaluate ovarian function, after superovulation with PMSG and hCG, the numbers of zygotes retrieved and embryo development rate were examined. Ovarian expressions of BMP15, GDF9, and C-KIT decreased with age. Follicle counts, numbers of retrieved zygotes, and embryo development rate were also significantly reduced in old mice over 30 weeks compared with young mice. These results indicate that these factors could be served as new potential biomarkers of ovarian aging.

Introduction

Ovarian aging gradually decreases both oocyte quantity and quality of the oocytes, and it is a fastidious cause in infertility treatment.[1] In recent years, the number of women who are delaying childbearing or marriage is constantly increasing, and solving ovarian aging is an important issue in fertility preservation and infertility treatment.

Serum anti-Mullerian hormone (AMH) levels and antral follicle count (AFC) and are being practically used as markers of ovarian aging as well as ovarian reserve in human.[2–4] AMH is commonly used to assess the extent of ovarian follicle depletion, to diagnose premature ovarian insufficiency, and to predict age at menopause.[5–7]

However, serum AMH level has some drawbacks in assessing ovarian aging and reserve. First, because AMH is produced by preantral and antral follicles, it does not reflect the true ovarian reserve, which is determined by the quantity of primordial follicle.[8] A recent study suggests that serum AMH cannot be guaranteed as s biomarker of ovarian reserve.[9] Second, although healthy and young women with poor ovarian response has a low serum AMH level, when embryo quality was not bad and

embryo transfer proceeded, a relatively good pregnancy outcome could be obtained.[5,10] This means that serum AMH level cannot reliably reflect oocyte quality in young healthy women. Third, age of peak AMH very varies widely among studies.[11] Therefore, threshold values of serum AMH need to be standardized to evaluate ovarian reserve by focusing on the number of resting primordial follicle and female age.

Various growth factors, cytokines, gonadal hormones (FSH, LH, and GnRH) highly coordinate normal ovarian function, and follicular development in an autocrine, para-crine, and/or endocrine manner.[12,13] The C-KIT/kit ligand (KITL) via stimulation of the C-KIT receptor plays an essential role in ovarian folliculogenesis and oogenesis in mammals.[14] The theca cell-derived C-KIT plays several roles in the establishment of primordial germ cells, the activation of primordial follicle, and oocyte growth and survival.[15,16] The expression of KITL has been shown to be influenced by intra-ovarian growth differentiation factor 9 (GDF9).[17] GDF9 is one of representative transforming growth factor-β (TGF-β) superfamily members with bone morphogenetic protein 15 (BMP15).[18,19] They are produced in oocytes, cumulus cells, and granulosa cells.[20–23] In addition, mRNA expressions of *Gdf9 and Bmp15* have been reported to be positively correlated with age of women, which critically influence ovarian reserve and aging.[23] A genome-wide study showed that gene mutations of *Bmp15 and Gdf9* are involved in human premature ovarian failure (POF).[24] These results strongly indicate that BMP15, GDF9, and C-KIT may play a potential role in the processes of ovarian aging. Therefore, this study examined ovarian expressions of BMP15, GDF9, and C-KIT according to age in female mice to determine whether these factors could be new potential biomarkers of ovarian aging.

Materials and methods

Animals and experiments

C57BL/6 inbred female and male mice were purchased from the Koatech Inc. (Gyunggi-do, Korea) and maintained in plastic cages under controlled conditions of temperature ($22 \pm 1^\circ$C) and a 12-h light/12-h dark cycle with a access to food and tap water ad libitum throughout the study. All mice were treated under the guidance for the Care and Use of Laboratory Animals of the National Institutes of Health. The written consent for all animal experiment was approved from the Institutional Review Board and Animal Care and Use Committee of Pusan National University Hospital.

Ovarian tissue collection

Both intact ovaries were collected from female mice aged from 10, 20, 30, and 40 weeks. The one ovary was immediately fixed in paraformaldehyde for further histological and immunohistochemical (IHC) analyses, and the other ovary was stored at –80°C until used for real-time PCR, and Western blotting.

RNA isolation and quantitative PCR

Total RNA was extracted with Trizol reagent (Invitrogen, Carlsbad, CA, USA) according to the manufacturer's instruction. Complementary DNA was synthesized from 1 μg of total RNA using AMV Reverse Transcriptase (Promega, Madison, WI, USA) and a random hexamer (Takara Bio, Inc., Otsu, Japan) at 42°C for 1 h followed by inactivation of the enzyme at 95°C for 5 min.

Template complementary DNA was subjected to PCR amplification using gene-specific primers. The primers used were as follows: 5′-TTGCTCCTCGTCTCTATACC-3′ (sense) and 5′-CTAGATGGCATGGTTGG-3′ (antisense) for BMP15; 5′-AGTGTGTTGACCATTGAAC C-3′ (sense) and 5′-GCACCTCGTAGCTA TCATGTC-3 (antisense) for GDF9; 5′-GCCTAG TCATTGTTGCA-3′ (sense) and 5′-CCCA AGTTTGTCTATGATGG-3′ (antisense) for C-KIT; and 5′-ACCACAGTCATGC ATCAC-3′ (sense) and 5′-TCCACCACCCTGTTGCTGTA-3′ (antisense) for glyceral-dehyde 3-phosphate dehydrogenase (GAPDH). Quantitative PCR (qPCR) was carried out using Light Cycle 480 SYBR Green I Master (Roche Diagnostics, Mannheim, Germany). The reaction conditions consisted of denaturation at 95°C for 10 min, followed by 40 cycles of 95°C for 10 s, 56°C for 5 s, and 72°C for 20 s. All experiments were performed in duplicate on each sample, each being repeated at least three times. The relative expression levels of mRNA in each sample were calculated using the ddCt method. The level of each mRNA sample was normalized to the expression levels of the housekeeping gene GAPDH. Fold change differences were represented relative to 10 weeks and each experimental group.

Western blot analysis

Proteins from each sample were extracted by mechanical homogenization of ovaries in the presence of NP-40 lysis (50 mM Tris-HCl (pH 7.5), 150 mM NaCl, 1% Nonidet P-40, and 1 mM ethylenediamine-tetraacetic acid) buffer supplemented with phosphatase inhibitors. Equal amounts of protein were separated by sodium dodecyl sulfate polyacrylamide gel electrophoresis (SDS-PAGE) and transferred to a polyvinylidenedifluoride (PVDF) membrane (Millipore, Bedford, MA, USA). The membranes were incubated in tris-buffered saline (TBS) containing 1% Tween 20 (TBS-T) supplemented with skim milk to block non-specific antibody binding. Each membrane was incubated with specific primary anti-mouse BMP15, GDF9, C-KIT antibody (Santa Cruz Biotechnology, Santa Cruz, USA). Actin antibody (Sigma, St Louis, MO, USA) was used as an internal control. After washing four times with TBS-T, the blotted membranes were incubated with horse-radish peroxidase-conjugated goat antibody (Santa Cruz Biotechnology) for 30 min at room temperature. After washing three times with TBS-T, protein bands were visualized using an enhanced chemiluminescence detection system using the manufacture's recommended procedure (Amersham Pharmacia Biotech, Piscataway, NJ, USA). Protein bands were quantified and normalized relative to Actin using ImageJ software (NIH, version 1.35d).

RNA extraction and RNA sequencing

Total RNA each sample was isolated from ovaries of 6- and 48-week-old mice and were isolated using an RNAprep pure plant total RNA extraction kit (Qiagen, Hilden, Germany) according to the manufacturer's protocols. For each library preparation, mRNA was used to synthesize cDNA libraries using the TruSeq RNA Sample Preparation Kit v2 (Illumina, San Diego, USA) following the manufacturer's protocols. Subsequently, these cDNA libraries were quantified using the qPCR Quantification Protocol Guide and qualified using an Agilent Technologies 2100 Bioanalyzer. To measure expression levels, RNA-Seq reads were mapped to the C57BL/6 mouse genome using TopHat. The expression level of each gene was calculated in in FPKM (Fragments PerKilobase of exon per Million fragments mapped) using Cufflinks. These FPKM values were added 1 and transformed by logarithm 2. All statistical analyses were performed using functions implemented in the statistical software packages R 3.1.2. The normalization of RNA-seq data were subjected to most widely adopted method. Differentially expressed genes were performed using the following filter criteria: |fold change (FC) | ≥ 2 and independent T-test raw p-value < 0.05. The FC is the ratio of the group mean values. Transcripts with at least a 1.7-FC were selected. All adjusted p-values were calculated using a Student's t-test, and adjusted for multiple testing using Benjamini-Hochberg Procedures.

Immunohistochemistry

Immunohistochemistry (IHC) was in accordance with the ImmPRESS[TM] HRP REAGENT KIT (Peroxidase) (Vector Laboratories, Burlingame, CA, USA). After deparaffinization and rehydration steps have been completed, antigen retrieval was carried out by microwave treatment in 0.01 M sodium citrate buffer (pH 6.0) at 95°C for 15 min. The specimens were washed three times with PBS, and endogenous peroxidase activity was denatured with 3% hydrogen peroxide in methanol for 10 min. The sections were incubated with antiserum at a dilution of 1:200 in BMP15 (ORB247897, Biorbyt, Cambridge, UK), 1: 100 in GDF9 (AF739, R&D Systems, MN, USA), and 1:100 in C-KIT (ORB10286, Biorbyt) for overnight. The sections were then washed and incubated for 15 min with the biotinylated secondary antibodies. Immunoreactive signals were detected using streptavidin-HRP and diaminobenzidine (DAB MapKit, Ventana). After preparation, positive expression was shown by brown DAB precipitate, and sections were observed with a Nikon ECLIPSE E800 photomicroscope (Nikon, Tokyo, Japan). Images were acquired using a Leica DM2500 system (Leica Microsystems, Germany). For quantification of IHC staining, mean immunoreactivity intensity for surviving follicle in an ovarian section was measured using ImageJ software (ImageJ) and ImageJ plug in IHC profiler. Images were changed to 8-bit grayscale type and inverted under "Edit" menu of ImageJ to lead to result of color deconvolution. After invert, the DAB-stained areas are bright and unstained areas are dark. The mean intensity was measured using "Measure" function under the "Analyze" menu of ImageJ. Positive cases were evaluated in at least 10 fields of each group.

Histological analysis of ovaries sections with hematoxylin and eosin

Ovaries were fixed in 4% paraformaldehyde at 4°C overnight. Sections (5 μm) of paraffin-embedded ovarian tissues were deparaffinized, rehydrated in graded alcohol, and stained with hematoxylin and eosin (H&E) using standard protocols. After mounting, H&E-stained sections were analyzed histologically under a digitlight microscope. Follicle counts of differential classifications were counted using a modified Pedersen's classification system.[25] The follicle stages were classified as morphologically normal follicles which were quantified according to these criteria. They were then classified into primordial, primary, secondary, antral follicles, graffian follicles or atresia follicles. Briefly, follicles were classified as primordial follicle, which contain an oocyte surrounded by a complete layer of flattened granulosa cells; as primary follicles which contain an oocyte surrounded by one layer of cuboidal granulosa cells; as secondary follicles which contain an oocyte surrounded by at least two layers of cuboidal granulosa cells; antral follicles if an antrum cavity was visualized between follicular cells; and graffian follicles if a follicle with complete antrum around oocyte. To avoid double counting of follicles, at least 10 sections were counted only when the nucleolus was identified. Follicular atresia is the breakdown of the ovarian follicles, which consist of the presence of apoptotic bodies in the granulosa cell layer, disorganized granulosa cells, a degenerating oocyte, or fragmentation of the oocyte nucleus.

Superovulation and culture of zygotes to the blastocyst stage

For superovulation, female mice aged 10, 20, 30, and 40 weeks were intraperitoneally injected with 0.1 ml of 5 IU of pregnant mare's serum gonadotropin (PMSG, Sigma-Aldrich), followed by injection of 5 IU of human chorionic gonadotropin (hCG, Sigma) approximately 48 h later. And then, the mice were immediately paired with an individual male. After 24 hours on the following morning, cumulus-enclosed one-cell embryos (zygotes) were collected from the oviductal ampulae of the mice confirmed vaginal plug, which were considered to be fertilized. The cumulus cells were denuded with 0.1% hyaluronidase (Sigma) in Dulbecco's phosphate buffer saline (dPBS; Gibco BRL, Grand Island, USA). Zygotes were pooled and only healthy zygotes were cultured in 20 μL drops of P1 medium (Irvine Inc., Santana, USA) with 10% Serum Substitute Supplement (SSS, Irvine Inc.) for the first two days and then blastocyst medium (Irvine Inc.) with 10% SSS for the next two days under paraffin-oil at 37°C in a 5% CO_2 incubator, and the media were changed daily.

Statistical analysis

All data were presented as a mean $\pm$ standard deviations (SDs), and statistical analysis was performed using an SPSS program (version 12.0). Statistical analysis for comparison of gene expression of BMP15, GDF9, and C-KIT was performed by Student's t-test. The number of zygotes retrieved and blastocyst formation rate were analyzed by one-way analysis of variance with post hoc multiple comparisons by Bonferroni-Dunn analysis. A p value of <0.05 was considered statistically significant.

Results

The expressions of *Bmp15*, *Gdf9*, and *C-KIT* mRNA were examined in the ovaries of each age by qRT-PCR. Expressions of these three factors were decreased in old mice aged 40 weeks compared with young mice aged 10 weeks with a significance ($p < 0.05$). Especially, GDF9 and C-KIT expressions were decreased in an age-dependent manner. However, unexpectedly, BMP15 expression peaked in 20-week-old mice and began to decrease thereafter (Figure 1).

Immunohistochemistry was carried out to evaluate the localized BMP15, GDF9, and C-KIT expression in the ovary. The expressions of BMP15 (Figure 2(a) to (d)) and C-KIT (Figure 2(i) to (l)) were localized in oocytes, granulosa cells, and stromal cells surrounding follicles of all follicles including primary, secondary, antral, and graffian follicles, while GDF9 (Figure 2(e) to (h)) was expressed only in the oocytes of antral and graffian follicles, but not in the stromal cells. The expressions of BMP15 and C-KIT were decreased in aged mice of 40 weeks (Figure 2(d) and (l), respectively) compared with young mice aged 10 weeks (Figure 2(a) and (i), respectively). C-KIT immunostaining was weak or absent in the stromal cells in aged mice of 40 weeks (Figure 2(l)). The expression of GDF9 showed a tendency to decrease more clearly in an age-dependent manner. The quantitative result of this immunohistochemistry is consistent with the observation qRT-PCR (Figure 2(m)).

Western blot was performed to confirm the quantitative protein expression of these factors in the ovary according to the age. Similar to mRNA expression and immunohistological results, protein expressions of BMP15, GDF9, and C-KIT by Western blot were also significantly decreased in old mice aged 40 weeks compared with young mice aged 10 weeks (Figure 3).

To determine whether the expression of these genes also differs with age in the transcriptome analysis, RNA-Seq was performed on ovaries of 6-week and 48-week-old mice. A total of 24,532 genes were screened, including 202 differentially expressed genes (DEGs) between 6-week and 48-week-old mice with |fold change|≥ 2 and t-test p-value < 0.05. In RNA sequencing analysis, three genes (BMP15, GDF9, and C-KIT) were selected from the DEGs between 6-week and 48-week-old mice groups to verify the qPCR data. As shown in Figure 4(a), the ovaries of 48-week-old mice significantly down-regulated the mRNA abundance BMP15 (p-value = 0.0081), GDF9 (p-value = 0.0091), and C-KIT (p-value = 0.0017). The results of the qPCR were similar to those of the RNA-seq data analysis (Figure 4(b)).

Numbers of primordial, primary, secondary, antral, graffian, and atretic follicles per ovary of mice aged 10 weeks to 40 weeks were examined by H&E staining (Figure 5(a) to (d)). The number of primordial follicles decreased in an age-dependent manner with significance ($p < 0.05$), and the number of primary to graffian follicles was also significantly lower in older mice (≥ 30 weeks old) than younger mice (≤ 10 weeks old) ($p < 0.05$). Atretic follicles had no age-related differences (Figure 5(e)). Severe degeneration and necrosis of granulosa cells were observed in older mice aged ≥ 30 weeks (Figure 5(c) and (d), black arrowhead) compared with young mice (Figure 5(a), open arrowhead).

In order to confirm whether mice used in this study fully reflects characteristics of aging-related natural ovarian aging, numbers of ovulated oocytes and embryo development rate were examined. The number of ovulated oocytes was measured by the number of zygotes retrieved collected
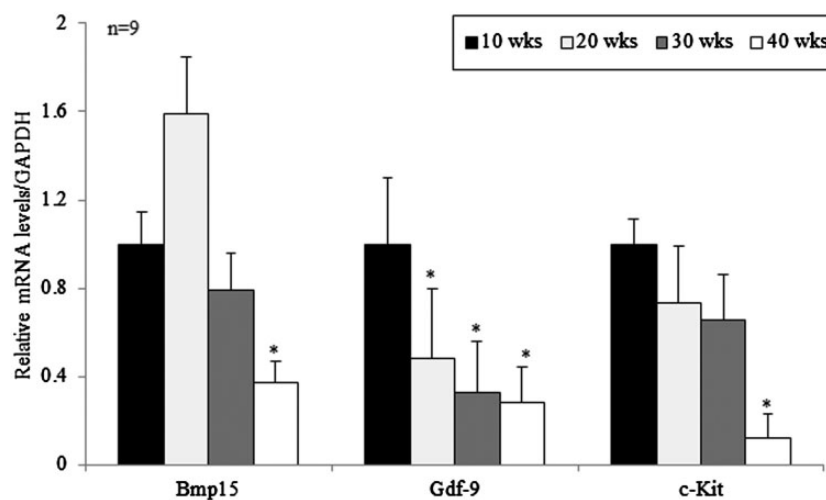
Figure 1. Relative mRNA expressions of *Bmp15*, *Gdf9*, and *C-KIT* in the ovaries of mice aged from 10 to 40 weeks. Levels of the mRNAs of *Bmp15*, *Gdf9*, and *C-KIT* were normalized to the amount of GAPDH per sample. Data are presented as mean $\pm$ standard deviation.*p < 0.05 (vs. 10 weeks old). GAPDH: glyceraldehyde 3-phosphate dehydrogenase.
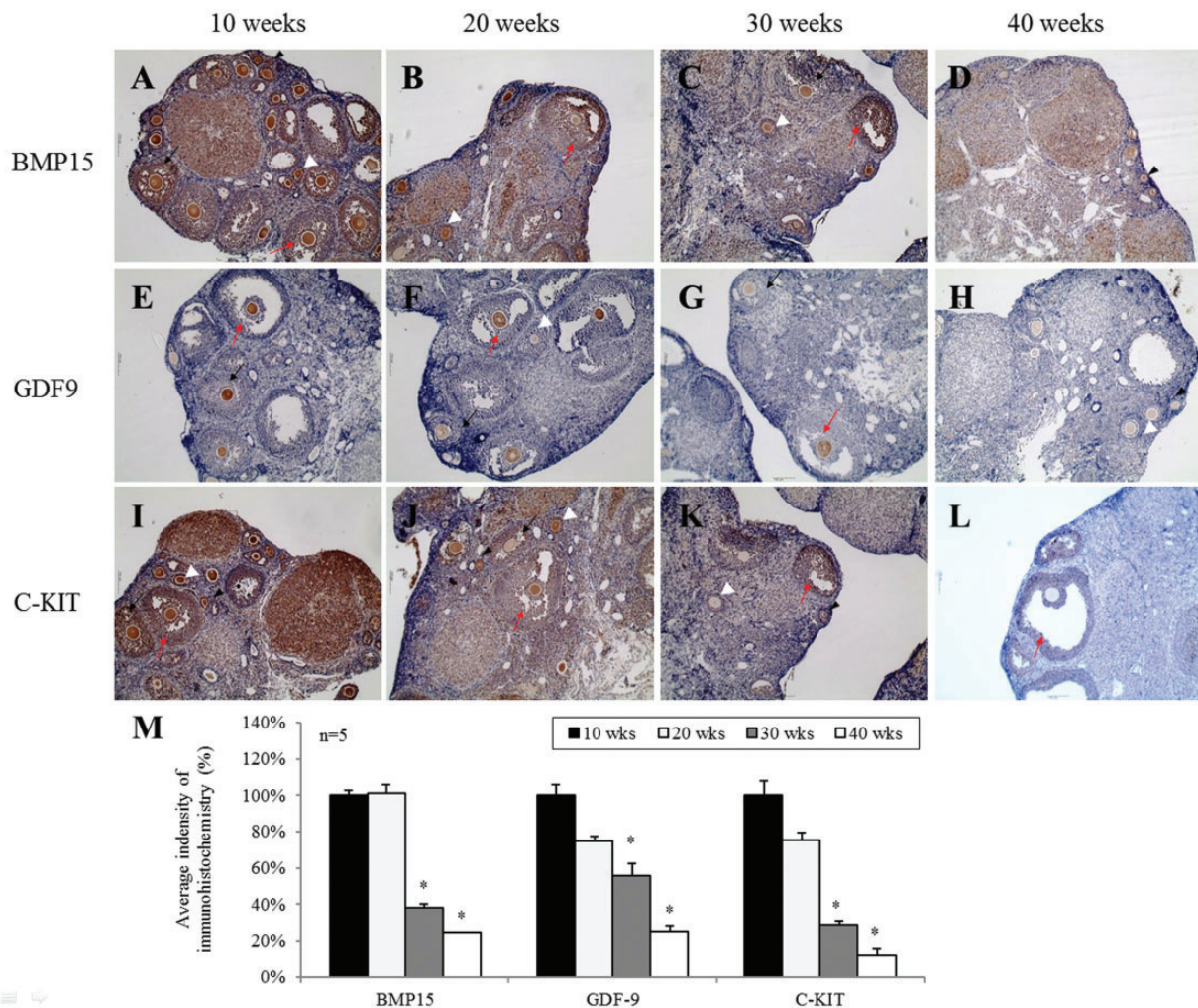
Figure 2. Immunohistochemistry of BMP15, GDF9, and C-KIT in the mouse ovaries according to age. (a, e, i) 10 weeks, (b, f, j) 20 weeks, (c, g, k) 30 weeks, and (d, h, l) 40 weeks of mice. Immunostainings with anti-BMP15 (a–d) and cv-Kit (i–l) antibodies were usually localized in oocyte and cumulus cells, whereas immunostaining with anti-GDF antibody (e–h) was detected just in the oocytes (brown). (m) Quantitative results of immunohistochemistry analysis. Five ovaries were used per age group and a total of 10 follicles per ovary were counted for analysis. The images are representative at a final magnification of ×100. Scale bar indicates 50 μm. Black arrowhead, white arrowhead, black arrow, and red arrow indicate oocytes of primary, secondary, antral, and graffian follicles, respectively. *p < 0.05 (vs. 10 weeks old). (A color version of this figure is available in the online journal.)

after mating with male mice, and the embryo development rate was observed up to blastocyst. The mean number of zygotes retrieved was decreased in an age-dependent manner, showing that the number of zygotes was 17.1 in 10 weeks, 17.2 in 20 weeks, 16.1 in 30 weeks, and 13.0 in 40 weeks. The mean percentages of fragmented zygotes was 33.3% in 40 weeks, which was significantly greater than those of 10 (9.1%) and 20 (12.3%) weeks. Embryo development rates to blastocyst was also significantly lower in older mice aged 30 and 40 weeks (7.8% and 6.4%) than young mice aged 10 and 20 weeks (47.9% and 22.2%) (Table 1).

Discussion

Several previous studies have suggested that BMP15, GDF9, and C-KIT could be useful biomarkers of ovarian aging in relation to female age. The true ovarian reserve and ovarian aging are really reflected by the number of primor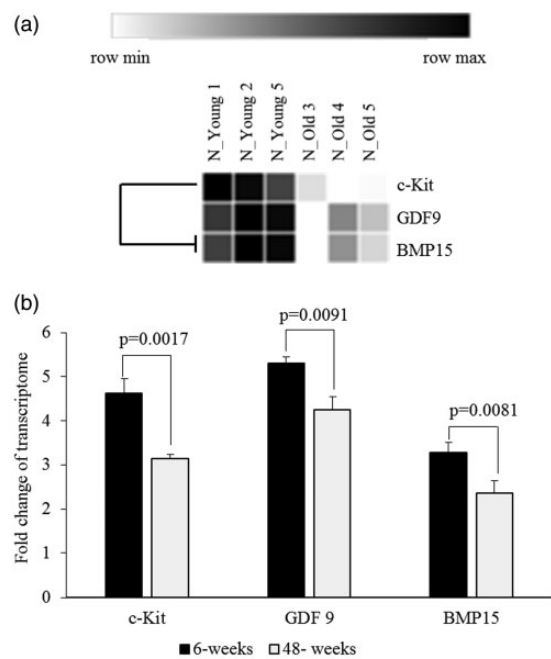dial follicles. The PI3K pathway is a fundamental signaling pathway that regulates primordial follicles activation,[26] and it is regulated by KL/C-KIT system. Kit signaling via PI3K promotes ovarian follicle maturation.[27] KL/C-KIT expression in granulosa cells is stimulated by BMP15 and GDF9.[17] BMP15 and GDF9 also play important roles in primordial follicle activation and follicular development.[28–31] The present study shows that ovarian expressions of BMP15, GDF9 and C-KIT decrease at mRNA and protein levels with age. This result suggests for the first time that these factors could be served as new potential biomarkers of ovarian aging.

This study showed a significant decreased ovarian mRNA and protein expressions of BMP15, GDF9, and C-KIT in aged mice (≥30 weeks old) compared with young mice (≤10 weeks old). Transcriptome analysis with RNA-Seq showed that a total of 202 differentially expressed genes (DEGs) were identified associated with ovarian aging among screening of 24,532 genes. Among them, expressions of *Bmp15, Gdf9,* and *C-KIT* were significantly declined age-associated decline at 48-week-old mice.
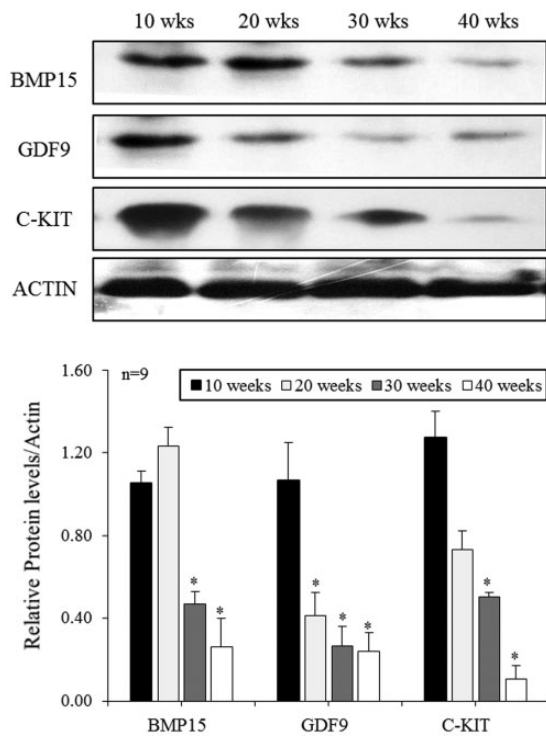
Figure 3. Protein expressions of BMP15, GDF9, and C-KIT in the ovaries of mice aged 10 to 40 weeks. Protein expression levels of BMP15, GDF9, and C-KIT were normalized to the amount of actin per sample. Relative protein densities were quantified using NIH-Image J software (version 1.35d). Data are presented as mean ± standard deviation. Results are representative of at least three independent experiments. *$p < 0.05$ (vs. 10 weeks old).

Figure 4. Expressions changes of *Bmp15*, *Gdf9* and *C-KIT* in transcriptome analysis using RNA-Seq for ovaries of mice aged 6 weeks and 48 weeks. (a) Heat-map results, (b) quantification of expression level of mRNA. Expressions of BMP15, GDF9, and C-KIT were significantly decreased in old mice compared with young mice.

Expression of GDP9 was age-dependently decreased. However, ovarian BMP15 expression showed an unexpected peak at 20 weeks and began to decrease significantly after 20 weeks old in an age-dependent manner. GDF9 has been suggested to reflect oocyte quality because its expression was found to be diminished in oocytes from old mice.[32] Abnormal expression of BMP15 and GDF9 was associated with the pathogenesis of woman ovarian disease such as POF. Elevation in *Bmp15* and *Gdf9* mRNA levels in cumulus granulosa cells was closely correlated with oocyte maturation, fertilization, embryo quality, and pregnancy outcome in women undergoing IVF-ET.[23] In addition, the mRNA expressions of *Bmp15 and Gdf9* were found to be positively associated with age,[23] which are known to importantly influence ovarian aging. As above, BMP15 and GDP alone or synergistically play an important role in control of ovarian function by regulating both granulosa cells fate and oocyte developmental competency.[33–35] However, these two factors have critical differences in the two ways. One is they have different signaling pathway. The other is that BMP15 has less essential role in mouse reproduction function compared with GDF9. As a result, the GDF9 null mice results in infertility with a block of follicular development, while mice lacking BMP15 were subfertile with normal folliculogenesis because they have normal follicular development but showed defects in ovulation and early embryonic development.[36] As shown in Figure 2 and Table 1, 20-week-old mice maintained follicular development similar to that of 10-week-old mice, with a slight decrease in egg production and developmental competency. These results speculate that BMP15 expression is at least maintained or increased until 20 weeks old, which shows normal follicular development, and then decreased. However, there was little research on ovarian BMP15 expression according to age yet, so further study is needed.

Many studies have reported that the KL/C-KIT system importantly regulates oogenesis and folliculogenesis such as initiation of follicular growth from the primordial pool, progression beyond the primary follicle stage, and modulation of the ability of oocytes to undergo cytoplasmic maturation in large antral follicles.[11,37,38] This result suggests that KL/C-KIT plays an important role in increasing the number of actively growing follicles and/or in regulating of primordial follicle maintenance. Nevertheless, no studies have yet been investigated the relation between ovarian C-KIT expression and female age. The present study clearly shows that ovarian expression of C-KIT decreases in an age-dependent manner.

In order for the expression patterns of these factors in this study to be useful potential biomarker of ovarian aging, first of all, the expression patterns of these factors should be associated with age-dependent decreased follicular development and ovarian function. Therefore, the present study carried out two experiments. One is the H&E stain of ovaries by age of mice, and the other is the evaluation of the number of ovulated oocytes and embryo development rate. As expected, the H&E stain showed that numbers of primordial, primary, secondary, antral, and graffian follicles were progressively decreased with increasing age. In addition, numbers of ovulated oocytes and blastocyst formation rate began to gradually decrease
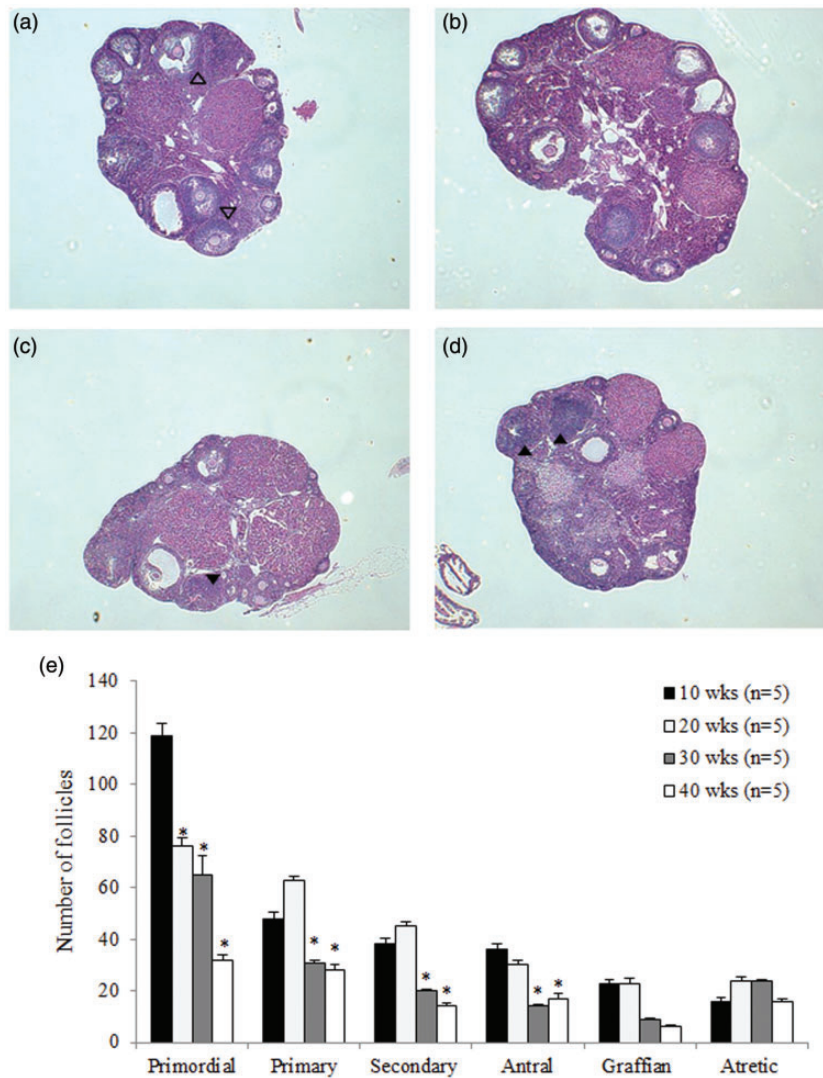
Figure 5. Representative hematoxylin and eosin (H&E) sections of ovaries from mice of different ages. (a) 10 weeks, (b) 20 weeks, (c) 30 weeks, and (d) 40 weeks old. (e) Numbers of primordial, primary, secondary, antral, graffian, and atretic follicles per ovary at different ages. Numbers of follicles from primordial to graffian follicles gradually reduced with increasing age. *p < 0.05 (vs. 10 weeks old). (A color version of this figure is available in the online journal.)

Table 1. Numbers of zygotes retrieved and embryo development to blastocyst.

Age of mice (weeks)	No. of mice provided	No. of zygotes retrieved	No. of zygotes retrieved/mouse	No. (%) of zygotes fragmented	No. of zygotes cultured	No. (%) of blastocysts
10	9	154	17.1±15.6[a]	14 (9.1)[a]	140	67 (47.9)[b]
20	9	155	17.2±18.3[a]	19 (12.3)[a]	136	30 (22.2)[b]
30	9	145	16.1±16.0	29 (20.0)	116	9 (7.8)
40	9	117	13.0±10.4	39 (33.3)	78	5 (6.4)

[a]P < 0.05 (vs. 40–45 weeks).
[b]P < 0.05 (vs. 30–35 weeks and 40–45 weeks).

from 30 weeks old. These results show that ovarian expression patterns of BMP15, GDF9, and C-KIT closely with age-related decline in ovarian function and follicular development potential.

Recently, many researchers have utilized the artificial follicular depletion models using mice to understand the mechanism of ovarian aging and menopause. They included Bax mouse, calorie-restricted rodent, 4-vinylcyclohexene dioxide (VCD)-treated rodent, or white spotting variant (Wu) mice model.[39–42] VCD-treated model was used to delete small preantral follicles and have been applied in infertility model in perimenopausal women or model of ovarian cancer.[43–44] Wu mice targets a point mutation in the C-KIT gene and results in a germ-cell deficiency, and they have been used as a genetic model in menopausal studies.[45] However, these models are made artificially

and do not really reflect natural ovarian aging process. Finn pointed out that there were no simple animal models to study natural physiology and pathology of ovarian aging and menopause.[46] Therefore, the present study used natural ovarian aging mouse model to evaluate the new potential biomarkers of ovarian aging.

However, the present study has some limitations. First, this study just investigated mRNA and protein expressions of BMP15, GDF9, and C-KIT in ovarian tissue. In order for these factors to be clinically used as real biomarkers of ovarian aging in human being, ovarian tissue sampling is required, but it is not easy like circulating blood sampling. Therefore, it is needed to examine the correlation between serum and ovarian expression level of these factors. Second, no comparison was made as to whether these factors are better as biomarkers of ovarian aging than AMH. Nevertheless, the present study is of great significance to understand that BMP15, GDF9, and C-KIT may be involved in ovarian aging processes and they could be available as new biomarkers for ovarian aging.

In conclusion, the present study shows that ovarian expressions of BMP15, GDF9, and C-KIT decrease with age, indicating that these factors could be served as new potential biomarkers of ovarian aging. Especially, the expression of GDF9 and C-KIT showed a significant decrease in an age-dependent manner, suggesting that GDF9 and C-KIT may be more useful biomarkers of ovarian aging. The identification of these potential biomarkers may contribute to the improvement in diagnosis and treatment of age-related fertility decline and premature ovarian insufficiency.

ORCID iD

Bo Sun Joo (iD) https://orcid.org/0000-0002-8214-3472

REFERENCES

1. Broekmans FJ, Knauff EA, teVelde ER, Macklon NS, Fauser BC. Female reproductive ageing: current knowledge and future trends. *Trends Endocrinol Metab* 2007;**18**:58–65
2. Knauff EA, Eijkemans MJ, Lambalk CB, ten Kate-Booij MJ, Hoek A, Beerendonk CC, Laven JS, Goverde AJ, Broekmans FJ, Themmen AP, de Jong FH, Fauser BC; Dutch Premature Ovarian Failure Consortium. Anti-Mullerian hormone, inhibin B, and antral follicle count in young women with ovarian failure. *J Clin Endocrinol Metab* 2009;**94**:786–92
3. Broekmans FJ, de Ziegler D, Howles CM, Gougeon A, Trew G, Olivennes F. The antral follicle count: practical recommendations for better standardization. *Fertil Steril* 2010;**94**:1044–51
4. Kokcu A. Premature ovarian failure from current perspective. *Gynecol Endocrinol* 2010;**26**:555–62
5. Lin PY, Huang FJ, Kung FT, Chiang HJ, Lin YJ, Lin YC, Lan KC. Evaluation of serum anti-Mullerian hormone as a biomarker of early ovarian aging in young women undergoing IVF/ICSI cycle. *Int J Clin Exp Pathol* 2014;**7**:6245–53
6. Kallio S, Aittomaki K, Piltonen T, Veijola R, Liakka A, Vaskivuo TE, Dunkel L, Tapanainen JS. Anti-Mullerian hormone as a predictor of follicular reserve in ovarian insufficiency: special emphasis on FSH-resistant ovaries. *Hum Reprod* 2012;**27**:854–60
7. Dolleman M, Depmann M, Eijkemans MJ, Heimensem J, Broer SL, van der Stroom EM, Laven JS, Van Rooij IA, Scheffer GJ, Peeters PH, van der Schouw YT, Lambalk CB, Broekmans FJ. Anti-Mullerian hormone is a more accurate predictor of individual time to menopause than mother's age at menopause. *Hum Reprod* 2014;**29**:584–91
8. Dewailly D, Andersen CY, Balen A, Broekmans F, Dilaver N, Fanchin R, Griesinger G, Kelsey TW, La Marca A, Lambalk C, Mason H, Nelson SM, Visser JA, Wallace WH, Anderson RA. The physiology and clinical utility of anti-Mullerian hormone in women. *Hum Reprod Update* 2014;**20**:370–85
9. Findlay JK, Hutt KJ, Hickey M, Anderson RA. What is the "ovarian reserve"? *Fertil Steril* 2015;**103**:628–30
10. Hagen CP, Vestergaard S, Juul A, Skakkebæk NE, Andersson AM, Main KM, Hjøllund NH, Ernst E, Bonde JP, Anderson RA, Jensen TK. Low concentration of circulating anti-Mullerian hormone is not predictive of reduced fecundability in young healthy women: a prospective cohort study. *Fertil Steril* 2012;**98**:1602–8
11. Cui L, Qin Y, Gao X, Geng L, Ding L, Qu Z, Zhang X, Chen ZJ. Antimüllerian hormone: correlation with age and androgenic and metabolic factors in women from birth to postmenopause. *Fertil Steril* 2016;**105**:481–5
12. Gougeon A. Regulation of ovarian follicular development in primates: facts and hypotheses. *Endocr Rev* 1996;**17**:121–55
13. Knight PG, Glister C. TGF-beta superfamily members and ovarian follicle development. *Reproduction* 2006;**132**:191–206
14. Thomas FH, Vanderhyden BC. Oocyte-granulosa cell interactions during mouse follicular development: regulation of kit ligand expression and its role in oocyte growth. *Reprod Biol Endocrinol* 2006;**12**:4–19
15. Carlsson IB, Laitinen MPE, Scott JE, Louhio H, Velentzis L, Tuuri T, Aaltonen J, Ritvos O, Winston RM, Hovatta O. Kit ligand and C-KIT are expressed during early human ovarian follicular development and their interaction is required for the survival of follicles in long-term culture. *Reproduction* 2006;**131**:641–9
16. Celestino JJH, Matos MHT, Saraiva MVA, Figueiredo JR. Regulation of ovarian folliculogenesis by kit ligand and the C-KIT system in mammals. *Anim Reprod* 2009;**6**:431–9
17. Gilchrist RB, Lane M, Thompson JG. Oocyte-secreted factors: regulators of cumulus cell function and oocyte quality. *Hum Reprod Update* 2008;**14**:159–77
18. Wang EA, Rosen V, Cordes P, Hewick RM, Kriz MJ, Luxenberg DP, Sibley BS, Wozney JM. Purification and characterization of other distinct bone-inducing factors. *Proc Natl Acad Sci USA* 1998;**85**:9484–8
19. Persani L, Rossetti R, Di Pasquale E, Cacciatore C, Fabre S. The fundamental role of bone morphogenetic protein 15 in ovarian function and its involvement in female fertility disorders. *Hum Reprod Update* 2014;**20**:869–83

20. Huang HY, Wang HS, Chan SH, Lee CL, Wang CW, Soong YK. Granulosa-lutein cell growth differentiation factor-9 (GDF-9) messenger RNA and protein expression in in vitro fertilization (IVF) cycles: relation to characteristics of ovulation induction and IVF. *Fertil Steril* 2009;**91**:1583–5

21. Shi FT, Cheung AP, Huang HF, Leung PC. Effects of endogenous growth differentiation factor 9 on activin A-induced inhibin B production in human granulosa-lutein cells. *J Clin Endocrinol Metab* 2009;**94**:5108–16

22. Margulis S, Abir R, Felz C, Nitke S, Krissi H, Fisch B. Bone morphogenetic protein 15 expression in human ovaries from fetuses, girls, and women. *Fertil Steril* 2009;**92**:1666–73

23. Li Y, Li RQ, Ou SB, Ren L, Wei LN1, Zhang QX, Yang DZ. Increased GDF9 and BMP15 mRNA levels in cumulus granulosa cells correlate with oocyte maturation, fertilization, and embryo quality in humans. *Reprod Biol Endocrinol* 2014;**12**:81

24. Persani L, Rossetti R, Cacciatore C. Genes involved in human premature ovarian failure. *J Mol Endocrinol* 2010;**45**:257–79

25. Pedersen T, Peters H. Proposal for a classification of oocytes and follicles in the mouse ovary. *J Reprod Fertil* 1968;**17**:555–7

26. Cantley LC. The phosphoinositide 3-kinase pathway. *Science* 2002;**296**:1655–7

27. John GB, Shidler MJ, Besmer P, Holland MK. Kit signaling via PI3K promotes ovarian follicle maturation but is dispensable for primordial follicle activation. *Dev Biol* 2009;**331**:292–9

28. Paulini F, Melo EO. The role of oocyte-secreted factors GDF9 and BMP15 in follicular development and oogenesis. *Reprod Domest Anim* 2011;**6**:354–61

29. Gilchrist RB, Ritter LJ, Cranfield M, Jeffery LA, Amato F, Scott SJ, Myllymaa S, Kaivo-Oja N, Lankinen H, Mottershead DG, Groome NP, Ritvos O. Immunoneutralization of growth differentiation factor 9 reveals it partially accounts for mouse oocyte mitogenic activity. *Biol Reprod* 2004;**71**:732–9

30. Trombly DJ, Woodruff TK, Mayo K. Roles for transforming growth factor beta superfamily proteins in early folliculogenesis. *Semin Reprod Med* 2009;**27**:14–23

31. Kedem A, Fisch B, Garor R, Ben-Zaken A, Gizunterman T, Felz C, Ben-Haroush A, Kravarusic D, Abir R. Growth differentiating factor 9 (GDF9) and bone morphogenetic protein 15 both activate development of human primordial follicles in vitro, with seemingly more beneficial effects of GDF9. *J Clin Endocrinol Metab* 2011;**96**:1246–54

32. Sharov AA, Falco G, Piao Y, Poosala S, Becker KG, Zonderman AB, Longo DL, Schlessinger D, Ko M. Effects of aging and calorie restriction on the global gene expression profiles of mouse testis and ovary. *BMC Biol* 2008;**6**:24

33. Sun RZ, Lei L, Cheng L, Jin ZF, Zu SJ, Shan ZY, Wang ZD, Zhang JX, Liu ZH. Expression of GDF-9, BMP-15 and their receptors in mammalian ovary follicles. *J Mol Histol* 2010;**41**:325–32

34. Peng J, Li Q, Wigglesworth K, Kattamuri C, Peterson RT, Eppig JJ, Thompson TB, Matzuk MM. Growth differentiation factor 9: bone morphogenetic protein 15 heterodimers are potent regulators of ovarian functions. *Proc Natl Acad Sci USA* 2013;**110**:E776–85

35. Belli M, Shimasaki S. Molecular aspects and clinical relevance of GDF9 and BMP15 in ovarian function. *Vitam Horm* 2018;**107**:317–48

36. McMahon HE, Hashimoto O, Mellon PL, Shimasaki S. Oocyte-specific overexpression of mouse bone morphogenetic protein-15 leads to accelerated folliculogenesis and an early onset of acyclicity in transgenic mice. *Endocrinology* 2008;**149**:2807–15

37. Driancourt MA, Reynaud K, Cortvrindt R, Smitz J. Roles of KIT and KIT LIGAND in ovarian function. *Rev Reprod* 2000;**5**:143–52

38. Hutt KJ, McLaughlin EA, Holland MK. Kit ligand and C-KIT have diverse roles during mammalian oogenesis and folliculogenesis. *Mol Hum Reprod* 2006;**12**:61–9

39. Wu JM, Zelinski MB, Ingram DK, Ottinger MA. Ovarian aging and menopause: current theories, hypotheses, and research models. *Exp Biol Med (Maywood)* 2005;**230**:818–28

40. Danilovich N, Ram Sairam M. Recent female mouse models displaying advanced reproductive aging. *Exp Gerontol* 2006;**41**:117–22

41. Smith ER, Xu XX. Ovarian ageing, follicle depletion, and cancer: a hypothesis for the aetiology of epithelial ovarian cancer involving follicle depletion. *Lancet Oncol* 2008;**9**:1108–11

42. Smith ER, Yeasky T, Wei JQ, Miki RA, Cai KQ, Smedberg JL, Yang WL, Xu XX. White spotting variant mouse as an experimental model for ovarian aging and menopausal biology. *Menopause* 2012;**19**:588–96

43. Haas JR, Christian PJ, Hoyer PB. Effects of impending ovarian failure induced by 4-vinyl-cyclohexene diepoxide on fertility in C57BL/6 female mice. *Comp Med* 2007;**57**:443–9

44. Laviolette LA, Ethier JF, Senterman MK, Devine PJ, Vanderhyden BC. Induction of a menopausal state alters the growth and histology of ovarian tumors in a mouse model of ovarian cancer. *Menopause* 2011;**18**:549–57

45. Kappeler CJ, Hoyer PB. 4-vinylcyclohexene diepoxide: a model chemical for ovotoxicity. *Syst Biol Reprod Med* 2012;**58**:57–62

46. Finn CA. Reproductive ageing and the menopause. *Int J Dev Biol* 2001;**45**:613–7